

# New Biodegradable Thermogelling Copolymers Having Very Low Gelation Concentrations

Xian Jun Loh,<sup>†,‡</sup> Suat Hong Goh,<sup>‡</sup> and Jun Li<sup>\*,†,§</sup>

*Institute of Materials Research and Engineering, National University of Singapore, 3 Research Link, Singapore 117602, Department of Chemistry, Faculty of Science, National University of Singapore, 3 Science Drive 3, Singapore 117543, and Division of Bioengineering, Faculty of Engineering, National University of Singapore, 9 Engineering Drive 1, Singapore 117576, Singapore*

*Received August 14, 2006; Revised Manuscript Received October 25, 2006*

New biodegradable multiblock amphiphilic and thermosensitive poly(ether ester urethane)s consisting of poly-[(*R*)-3-hydroxybutyrate] (PHB), poly(ethylene glycol) (PEG), and poly(propylene glycol) (PPG) blocks were synthesized, and their aqueous solutions were found to undergo a reversible sol–gel transition upon temperature change at very low copolymer concentrations. The multiblock poly(ether ester urethane)s were synthesized from diols of PHB, PEG, and PPG using 1,6-hexamethylene diisocyanate as a coupling reagent. The chemical structures and molecular characteristics of the copolymers were studied by GPC, <sup>1</sup>H NMR, <sup>13</sup>C NMR, and FTIR. The thermal stability of the poly(PEG/PPG/PHB urethane)s was studied by thermogravimetry analysis (TGA), and the PHB contents were calculated based on the thermal degradation profile. The results were in good agreement with those obtained from the <sup>1</sup>H NMR measurements. The poly(PEG/PPG/PHB urethane)s presented better thermal stability than the PHB precursors. The water soluble poly(ether ester urethane)s had very low critical micellization concentration (CMC). Aqueous solutions of the new poly(ether ester urethane)s underwent a sol–gel–sol transition as the temperature increased from 4 to 80 °C, and showed a very low critical gelation concentration (CGC) ranging from 2 to 5 wt %. As a result of its multiblock architecture, a novel associated micelle packing model can be proposed for the sol–gel transition for the copolymer gels of this system. The new material is thought to be a promising candidate for injectable drug systems that can be formulated at low temperatures and forms a gel depot *in situ* upon subcutaneous injection.

## Introduction

The synthesis of biodegradable thermogelling polymers have attracted much attention because of their potential applications for drug delivery and tissue engineering.<sup>1–6</sup> Bioactive agents can be incorporated in the sol state at low temperatures. This formulation can be injected into the body where the higher body temperature would lead to the formation of a gel depot. This depot can be used for the controlled release of the bioactive agents. Biodegradable linkages introduced into the polymer backbone would facilitate the degradation of the copolymer into smaller fragments and subsequent removal of the polymer from the body.

As an example of thermogelling polymers, the triblock copolymers of poly(ethylene glycol)-poly(propylene glycol)-poly(ethylene glycol) (PEG-PPG-PEG) have been widely investigated for controlled drug delivery,<sup>6–7</sup> wound covering,<sup>8</sup> and chemosensitizing for cancer therapy.<sup>9</sup> However, they generally have a high critical gelation concentration (CGC) (15–20 wt % or above), exhibiting poor resilience as well as having the burst effect of the release of bioactive agents. These shortcomings have made this system unsuitable for many biomedical applications.<sup>10–11</sup> Moreover, PEG-PPG-PEG triblock copolymers are non-biodegradable and have been reported to induce

hyperlipidemia and increase the plasma level of cholesterol in rabbits and rats, suggesting that its use in the human body may not be an attractive option.<sup>12–14</sup>

Attempts have been made to lower the CGCs of EPE triblock copolymers. By grafting PEG-PPG-PEG triblocks to poly(acrylic acid), polymers having very low CGCs (0.1 wt %) have been synthesized.<sup>15–18</sup> However, these polymers are non-biodegradable, and the excretion from the body could be difficult. High molecular weight multiblock PEG-PPG-PEG triblock copolymers with a short junction linkages have been synthesized and found to exhibit lower CGCs than PEG-PPG-PEG triblock copolymers.<sup>19–20</sup> Cohn et al. have synthesized reverse thermogelling multiblock copolymers based on PEG, PPG, and PCL.<sup>21</sup> These biodegradable copolymers exhibited CGCs of 10 wt %. Interestingly, this work showed that the incorporation of oligo-caprolactone segments lowered the CGCs of the copolymers as compared with the PPG-PEG multiblock copolymers. The viscosities of the gels were also lowered compared with the PPG-PEG multiblock copolymers. On the other hand, PEG-PPG-PEG analogues were developed where the middle PPG block was replaced by a biodegradable polyester such as poly(ε-caprolactone) or poly(L-lactide), which are of great significance in biomedical applications because of their biodegradability. However, their CGCs are at a similar range of PEG-PPG-PEG triblock copolymers.<sup>22</sup>

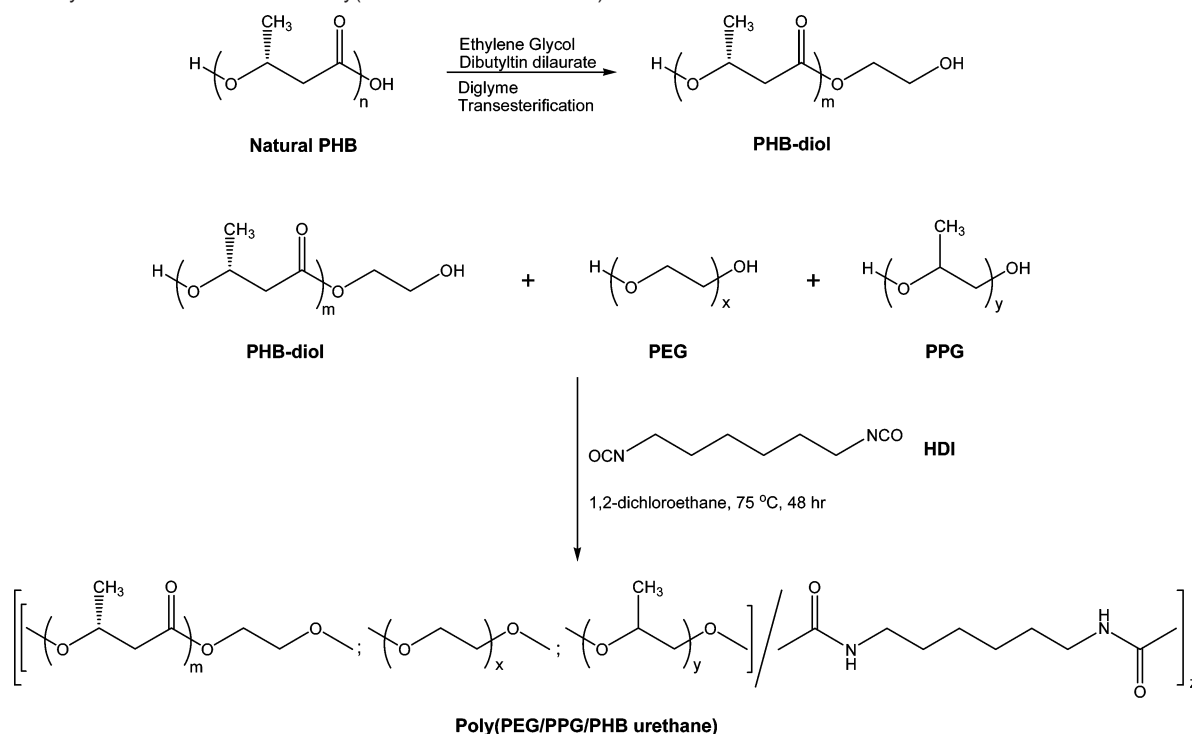
Poly[(*R*)-3-hydroxybutyrate] (PHB) is a natural biodegradable polyester, which is highly crystalline and hydrophobic, showing a greater hydrophobicity than either poly(lactic acid) or poly(ε-caprolactone).<sup>23</sup> Herein we hypothesize that incorporating PHB segments into a PEG-PPG block copolymer would allow

\* To whom correspondence should be addressed at Division of Bioengineering, National University of Singapore. Phone: +65-6516-7273 or 6874-8376. Fax: +65-6872-3069. E-mail: bielj@nus.edu.sg or jun-li@imre.a-star.edu.sg.

<sup>†</sup> Institute of Materials Research and Engineering.

<sup>‡</sup> Department of Chemistry, Faculty of Science.

<sup>§</sup> Division of Bioengineering, Faculty of Engineering.

**Scheme 1.** Synthesis of PHB-diol and Poly(PEG/PPG/PHB urethane)s

the formation of extra physical cross-linking in the hydrogel, increasing its resilience. Additionally, PHB segments would provide the biodegradable segments in the polymer backbone. In this work, we have designed a series of novel thermogelling high molecular weight amphiphilic multiblock poly(ether ester urethane)s consisting of PEG, PPG, and PHB blocks (Scheme 1). We have shown that this simple synthetic method produces thermogelling copolymers with very low CGCs and tunable properties, which may be potentially applied as an *in situ* forming biodegradable gel depot suitable for sustained drug delivery.

### Experimental Section

**Materials.** Natural source poly[(*R*)-3-hydroxybutyrate] (PHB) was supplied by Aldrich and purified by dissolving in chloroform followed by filtration and subsequent precipitation in hexane before use. The  $M_n$  and  $M_w$  of the purified PHB were  $8.7 \times 10^4$  and  $2.3 \times 10^5$ , respectively. Poly(ethylene glycol) (PEG) and poly(propylene glycol) (PPG) with  $M_n$  of ca. 2000 was purchased from Aldrich. Purification of the PEG was performed by dissolving in dichloromethane followed by precipitation in diethyl ether and vacuum-dried before use. Purification of PPG was performed by washing in hexane three times and vacuum-drying before use. The  $M_n$  and  $M_w$  of PEG were found to be 1890 and 2060, respectively. The  $M_n$  and  $M_w$  of PPG were found to be 2180 and 2290, respectively. Bis(2-methoxyethyl) ether (diglyme, 99%), ethylene glycol (99%), dibutyltin dilaurate (95%), 1,6-hexamethylene diisocyanate (HDI) (98%), methanol, diethyl ether, 1,2-dichloroethane (99.8%), and 1,6-diphenyl-1,3,5-hexatriene (DPH) were purchased from Aldrich. Diglyme was dried with molecular sieves, and 1,2-dichloroethane was distilled over  $\text{CaH}_2$  before use. PEG-PPG-PEG triblock copolymer with a chain composition of  $\text{EG}_{100}\text{PG}_{65}\text{EG}_{100}$  (also known as Pluronic F127) was purchased from Aldrich and used as received.

**Synthesis of Poly(PEG/PPG/PHB urethane)s.** Telechelic hydroxylated PHB (PHB-diol) prepolymers with various molecular weight were prepared by transesterification between the natural source PHB and ethylene glycol using dibutyltin dilaurate in diglyme as reported previously.<sup>24–26</sup> The yields were about 80%. Poly(PEG/PPG/PHB urethane)s were synthesized from PHB-diol, PEG, and PPG with molar

ratios of PEG/PPG fixed at 2:1 and PHB content ranging from 5 to 20 mol % (calculated from the  $M_n$  of PHB-diol) using HDI as a coupling reagent. The amount of HDI added was equivalent to the reactive hydroxyl groups in the solution. Typically, 0.064 g of PHB-diol ( $M_n = 1070$ ,  $6.0 \times 10^{-5}$  mol), 1.44 g of PEG ( $M_n = 1890$ ,  $7.6 \times 10^{-4}$  mol), and 0.82 g of PPG ( $M_n = 2180$ ,  $3.8 \times 10^{-4}$  mol) were dried in a 250-mL two-neck flask at 50 °C under high vacuum overnight. Then, 20 mL of anhydrous 1,2-dichloroethane was added to the flask, and any trace of water in the system was removed through azeotropic distillation with only 1 mL of 1,2-dichloroethane being left in the flask. When the flask was cooled down to 75 °C, 0.20 g of HDI ( $1.2 \times 10^{-3}$  mol) and two drops of dibutyltin dilaurate ( $\sim 8 \times 10^{-3}$  g) were added sequentially. The reaction mixture was stirred at 75 °C under a nitrogen atmosphere for 48 h. The resultant copolymer was precipitated from diethyl ether and further purified by redissolving into 1,2-dichloroethane followed by precipitation in a mixture of methanol and diethyl ether to remove remaining dibutyltin dilaurate. A series of poly(PEG/PPG/PHB urethane)s with different compositions of PHB were prepared, and their number-average molecular weight and polydispersity values are given in Table 1. The yield was 80% and above after isolation and purification.  $^1\text{H}$  NMR ( $\text{CDCl}_3$ ) of poly(PEG/PPG/PHB urethane)s EPH2:  $\delta$  (ppm) 1.14 ( $\text{O}(\text{CH}_3)\text{CHCH}_2\text{O}$ ), 1.26 ( $\text{O}(\text{CH}_3)\text{CHCH}_2\text{CO}$ ), 1.32 ( $\text{OOCNHCH}_2\text{CH}_2\text{CH}_2\text{CH}_2\text{CH}_2\text{CH}_2\text{NHCOO}$ ), 1.48 ( $\text{OOCNHCH}_2\text{CH}_2\text{CH}_2\text{CH}_2\text{CH}_2\text{CH}_2\text{NHCOO}$ ), 2.44–2.63 ( $\text{O}(\text{CH}_3)\text{CHCH}_2\text{CO}$ ), 3.13 ( $\text{OOCNHCH}_2\text{CH}_2\text{CH}_2\text{CH}_2\text{CH}_2\text{CH}_2\text{NHCOO}$ ), 3.41 ( $\text{O}(\text{CH}_3)\text{CHCH}_2\text{O}$ ), 3.46 ( $\text{O}(\text{CH}_3)\text{CHCH}_2\text{O}$ ), 3.64 ( $\text{OCH}_2\text{CH}_2\text{O}$ ), 4.20 ( $\text{OOCNHCH}_2\text{CH}_2\text{CH}_2\text{CH}_2\text{CH}_2\text{CH}_2\text{NHCOO}$ ), 5.21–5.29 ( $\text{O}(\text{CH}_3)\text{CHCH}_2\text{CO}$ ).  $^{13}\text{C}$  NMR of EPH2 ( $\text{CDCl}_3$ ) of poly(PEG/PPG/PHB urethane)s:  $\delta$  (ppm) 17.77 ( $\text{O}(\text{CH}_3)\text{CHCH}_2\text{O}$ ), 20.14 ( $\text{O}(\text{CH}_3)\text{CHCH}_2\text{CO}$ ), 26.69 ( $\text{OOCNHCH}_2\text{CH}_2\text{CH}_2\text{CH}_2\text{CH}_2\text{NHCOO}$ ), 30.26 ( $\text{OOCNHCH}_2\text{CH}_2\text{CH}_2\text{CH}_2\text{CH}_2\text{CH}_2\text{NHCOO}$ ), 41.20 ( $\text{O}(\text{CH}_3)\text{CHCH}_2\text{CO}$ ), 64.18 ( $\text{OOCNHCH}_2\text{CH}_2\text{CH}_2\text{CH}_2\text{CH}_2\text{CH}_2\text{NHCOO}$ ), 67.99 ( $\text{O}(\text{CH}_3)\text{CHCH}_2\text{CO}$ ), 70.94 ( $\text{OCH}_2\text{CH}_2\text{O}$ ), 73.56 ( $\text{O}(\text{CH}_3)\text{CHCH}_2\text{O}$ ), 75.72 ( $\text{O}(\text{CH}_3)\text{CHCH}_2\text{O}$ ), 156.82 ( $\text{OOCNHCH}_2\text{CH}_2\text{CH}_2\text{CH}_2\text{CH}_2\text{CH}_2\text{NHCOO}$ ), 169.98 ( $\text{O}(\text{CH}_3)\text{CHCH}_2\text{CO}$ ).

**Molecular Characterization.** Gel permeation chromatography (GPC) analysis was carried out with a Shimadzu SCL-10A and LC-8A system equipped with two Phenogel 5  $\mu\text{m}$  50 and 1000 Å columns (size: 300  $\times$  4.6 mm) in series and a Shimadzu RID-10A refractive index detector. THF was used as eluent at a flow rate of 0.30 mL/min

**Table 1.** Molecular Characteristics of Poly(PEG/PPG/PHB urethane)s

copolymer <sup>a</sup>	$M_n$ of PHB used <sup>b</sup> (g mol <sup>-1</sup> )	feed ratio (wt %)			composition in copolymer (wt %) <sup>c</sup>			copolymer characteristics		
		PHB	PEG	PPG	PHB	PEG	PPG	$M_n^b (\times 10^3)$	$M_w/M_n^b$	cmc <sup>d</sup> (g/mL)
EPH1	1070	2.8	61.7	35.5	2.1	64.0	33.9	50.6	1.56	$9.79 \times 10^{-4}$
EPH2	1070	5.6	59.9	34.5	5.1	57.0	37.9	45.5	1.38	$8.69 \times 10^{-4}$
EPH3	1070	8.7	58.0	33.4	8.1	56.3	35.7	42.5	1.37	$5.16 \times 10^{-4}$
EPH4	1070	11.8	55.9	32.2	11.4	61.6	27.0	37.8	1.16	- <sup>e</sup>
EPH5	2800	6.9	59.1	34.0	7.1	63.3	29.7	39.2	1.18	$8.88 \times 10^{-4}$
EPH6	2800	13.6	54.8	31.6	12.7	59.0	28.3	30.0	1.20	- <sup>e</sup>

<sup>a</sup> Poly(PEG/PPG/PHB urethane)s are denoted EPH, E for PEG, P for PPG and H for PHB. The  $M_n$  of PEG and PPG used for the copolymer synthesis was 1890 and 2180 g mol<sup>-1</sup>, respectively. <sup>b</sup> Determined by GPC. <sup>c</sup> Calculated from <sup>1</sup>H NMR results. <sup>d</sup> Critical micellization concentration (cmc) in water determined by the dye solubilization technique at 25 °C. <sup>e</sup> Copolymers not water-soluble.

at 40 °C. Monodispersed poly(ethylene glycol) standards were used to obtain a calibration curve. The <sup>1</sup>H NMR (400 MHz) and <sup>13</sup>C NMR (100 MHz) spectra were recorded on a Bruker AV-400 NMR spectrometer at room temperature. The <sup>1</sup>H NMR measurements were carried out with an acquisition time of 3.2 s, a pulse repetition time of 2.0 s, a 30° pulse width, 5208 Hz spectral width, and 32K data points. Chemical shift was referred to the solvent peaks ( $\delta$  = 7.3 ppm for CHCl<sub>3</sub>). Fourier transform infrared (FTIR) spectra of the polymer films coated on CaF<sub>2</sub> plate were recorded on a Bio-Rad 165 FT-IR spectrophotometer; 64 scans were signal-averaged with a resolution of 2 cm<sup>-1</sup> at room temperature.

**Thermal Analysis.** Thermogravimetric analyses (TGA) were carried out on a TA Instruments SDT 2960. Samples were heated at 20 °C min<sup>-1</sup> from room temperature to 800 °C in a dynamic nitrogen atmosphere (flow rate = 70 mL min<sup>-1</sup>).

**Critical Micellization Concentration (CMC) Determination.** The CMC values were determined by using the dye solubilization method.<sup>27,28</sup> The hydrophobic dye 1,6-diphenyl-1,3,5-hexatriene (DPH) was dissolved in methanol with a concentration of 0.6 mM. 20  $\mu$ L of this solution was mixed with 2.0 mL of copolymer aqueous solution with concentrations ranging from 0.0001 to 0.5 wt % and equilibrated overnight at 4 °C. A UV-vis spectrophotometer was used to obtain the UV-vis spectra in the range of 330–430 nm at 25 °C. The CMC value was determined by the plot of the difference in absorbance at 378 nm and at 400 nm ( $A_{378} - A_{400}$ ) versus logarithmic concentration.

**Sol-Gel Transition.** The sol-gel transition was determined by a test tube inverting method with temperature increments of 2 °C per step.<sup>22a, 29</sup> Each sample of a given concentration was prepared by dissolving the polymer in distilled water in a 2-mL vial. After equilibration at 4 °C for 24 h, the vials containing samples were immersed in a water bath at a constant designated temperature for 15 min. The gelation temperature was characterized by the formation of a firm gel that remained intact when the tube was inverted by 180°.<sup>30</sup>

**Viscosity Measurements.** Viscosities of the hydrogels were measured at 25 °C using a Brookfield HADV-III+ digital viscometer coupled to a temperature-controlling unit. The small sample adapter SSA 15/7R was used. The revolution rate of the spindle was set at 20 cycles min<sup>-1</sup> and shear rate was set at 9.6 s<sup>-1</sup>.

## Results and Discussion

**Synthesis and Characterization of Poly(PEG/PPG/PHB urethane)s.** Previously, we reported the synthesis and biodegradation behavior of amphiphilic multiblock poly(ether ester urethane)s consisting of PEG and PHB blocks.<sup>24–26</sup> These water-insoluble copolymers could not undergo a sol-gel transition and were non-thermosensitive. However, in this study, water-soluble and thermosensitive poly(PEG/PPG/PHB urethane)s were synthesized, and for the first time PHB has been incorporated into a thermogelling copolymer, to enhance the gel properties as well as to make the copolymers biodegradable.

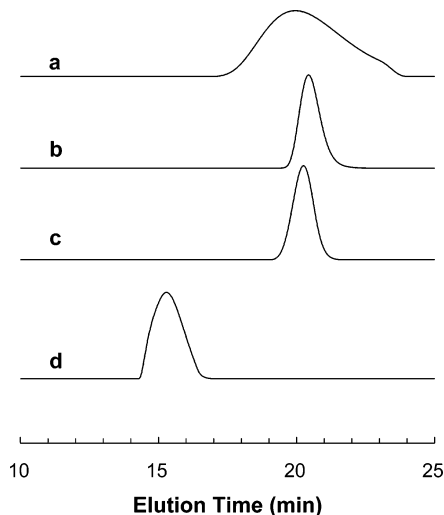


**Figure 1.** GPC diagrams of EPH2 and its PHB, PEG, and PPG precursors: (a) PHB-diol ( $M_n$  1080); (b) PEG ( $M_n$  1890); (c) PPG ( $M_n$  2180); (d) EPH2 ( $M_w$   $62.8 \times 10^3$ ,  $M_n$   $45.5 \times 10^3$ ,  $M_w/M_n$  1.38).

Telechelic hydroxylated PHB (PHB-diol) with lower molecular weight were obtained through transesterification between high-molecular-weight natural source PHB and ethylene glycol using dibutyltin dilaurate as catalyst.<sup>24</sup> The transesterification reaction was allowed to proceed for a few hours to overnight to produce PHB-diols with  $M_n$  of 1070 and 2800, respectively, as determined by GPC. The reaction of hydroxyl groups of PHB-diol, PEG, and PPG with isocyanate of 1,6-hexamethylene diisocyanate (HDI) in the presence of dibutyltin dilaurate led to formation of poly(PEG/PPG/PHB urethane)s. The procedures for the synthesis of PHB-diol and poly(PEG/PPG/PHB urethane)s are presented in Scheme 1. Owing to the moisture sensitive nature, any trace of water in the system was removed through azeotropic distillation, and the reaction was carried out in dried 1,2-dichloroethane under a nitrogen atmosphere. The target poly(PEG/PPG/PHB urethane)s were isolated and purified from the reaction mixture by repeated precipitation from a mixture of methanol and diethyl ether.

A series of random multiblock poly(PEG/PPG/PHB urethane)s with different amounts of PHB incorporated were synthesized, and their molecular weights and molecular weight distributions were determined by GPC (Table 1). A typical GPC chromatograph for one of the poly(PEG/PPG/PHB urethane)s together with its corresponding precursors is shown in Figure 1. The observation of unimodal peak in GPC chromatograph of the purified poly(PEG/PPG/PHB urethane) with non-overlapping nature with those of corresponding precursors indicates that a complete reaction took place with no unreacted precursor

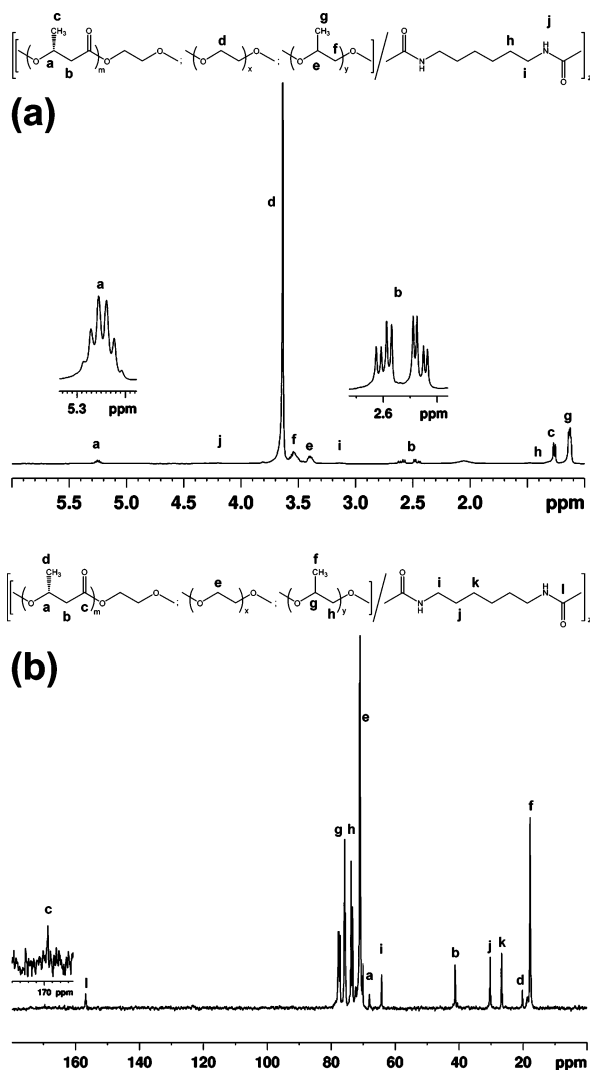


**Figure 2.** (a) 400 MHz <sup>1</sup>H NMR and (b) 100 MHz <sup>13</sup>C NMR spectra of EPH2 in CDCl<sub>3</sub>.

remained.<sup>24–26</sup> All the poly(PEG/PPG/PHB urethane)s synthesized had narrow molecular weight distribution and high molecular weight, with polydispersity ranging from 1.16 to 1.56 and  $M_n$  from  $3.00 \times 10^4$  to  $5.06 \times 10^4$ . The results are tabulated in Table 1.

The chemical structure of poly(PEG/PPG/PHB urethane)s was verified by <sup>1</sup>H NMR and <sup>13</sup>C NMR spectroscopy (Figure 2a,b). Figure 2a shows the <sup>1</sup>H NMR spectrum of EPH2 in CDCl<sub>3</sub>, in which all proton signals belonging to both PHB, PEG, and PPG segments are confirmed. Signals corresponding to methylene protons in repeated units of PEG segments are observed at 3.64 ppm, the signals at 5.25 ppm are assigned to methine protons in the repeated unit of PHB segments,<sup>24–26</sup> the signals at 1.14 ppm are assigned to the methyl protons of PPG. As the content of HDI among the starting materials is below 1 wt %, the compositions of the poly(PEG/PPG/PHB urethane)s could be determined from the integration ratio of resonances at 1.14, 3.64, and 5.25 ppm within the limits of <sup>1</sup>H NMR precision, and the results are shown in Table 1.

The <sup>13</sup>C NMR was used to ascertain the chemical composition of the poly(PEG/PPG/PHB urethane)s. The peak assignments of the copolymers were performed by comparison with the <sup>13</sup>C NMR spectra of the precursors. Figure 2b shows the <sup>13</sup>C NMR spectra of EPH2 in CDCl<sub>3</sub>. Briefly, peaks at 17.77 (methyl C), 73.56 (methylene C), and 75.72 ppm (methine C) are assigned to the PPG moiety. A peak at 70.94 ppm is assigned to the

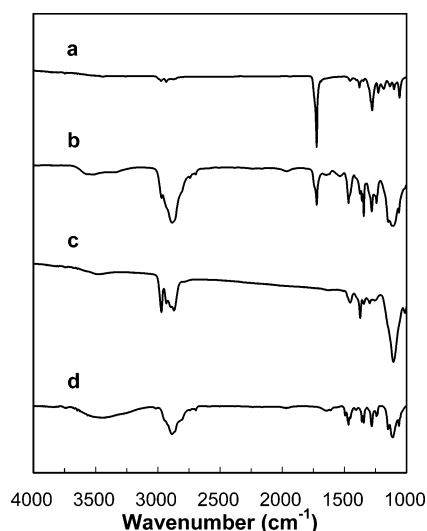


**Figure 3.** FTIR spectra of EPH2 and its PHB, PEG, and PPG precursors: (a) PHB-diol ( $M_n$  1080); (b) EPH2; (c) PPG ( $M_n$  2180); (d) PEG ( $M_n$  1890).

methylene C of the PEG segment. Peaks at 20.14 (methyl C), 41.20 (methylene C), 67.99 (methine C), and 169.98 ppm (carbonyl C) are attributed to the PHB segment. In addition, peaks due to the HDI junction unit could be observed in the spectra (26.69, 30.26, 64.18, and 156.82 ppm).

A <sup>13</sup>C NMR spectrum of hexamethylene diisocyanate was obtained, and the carbonyl carbon peak was observed at 122.85 ppm. After the polymerization reaction, the <sup>13</sup>C peak of the carbonyl carbon of the newly formed urethane linkage was observed at 156.82 ppm. This shift was attributed to the attachment of the hydroxyl groups to the isocyanate functional groups in the formation of the urethane linkage (NCO → NHCOO). This observation, together with the concomitant increase in the molecular weight of the copolymers indicates that the polycondensation reaction was successful.

FTIR is useful in the characterization of the functional groups present in the polymer. As a typical example, Figure 3 shows FTIR spectra of EPH2 and its PEG, PPG, and PHB precursors. For PPG (Figure 3c) and PEG (Figure 3d), the characteristic C—O—C stretching vibration of the repeated OCH<sub>2</sub>CH<sub>2</sub> units is observed at 1102 cm<sup>-1</sup>. An intensive carbonyl stretching band at 1723 cm<sup>-1</sup> characterizes the FTIR spectrum of pure PHB-diol as shown in Figure 3a. It is clearly seen that in Figure 3b, all the characteristic absorptions for PHB-diol, PEG, and PPG appear in the spectrum of EPH2, which confirms the presence of the three segments in the poly(PEG/PPG/PHB urethane)s. Furthermore, it can be seen in the profile of EPH2 that the peak ascribed to the NCO stretching was not observed in the region around 2200 cm<sup>-1</sup>. This provides evidence that the isocyanate groups of the junction units have been reacted and are not present in the polymer product. These observations, together with the aforementioned evidence (GPC and NMR results) provide a solid justification for the successful synthesis of the multiblock copolymers.

**Thermal Properties.** The thermal stability of poly(PEG/PPG/PHB urethane)s was evaluated using thermogravimetric analysis (TGA). Figure 4 shows the TGA scan results for EPH2 compared with its PHB, PEG, and PPG precursors. The degradation of pure PHB-diol starts at 218 °C and completes at 295 °C (Figure 4a), and PPG starts to degrade at 350 °C (Figure 4c) while that of pure PEG starts at 400 °C (Figure 4b). EPH2 undergoes a three-step thermal degradation with the first step occurring between 227 and 303 °C and the second



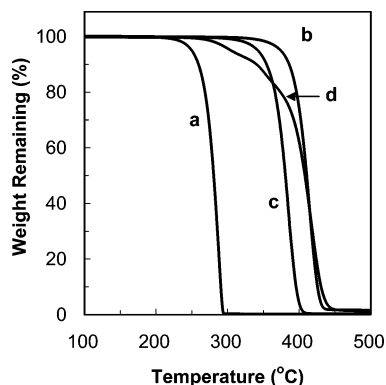


**Figure 4.** TGA curves of EPH2 and its PHB, PEG and PPG precursors: (a) PHB-diol ( $M_n$  1080); (b) PEG ( $M_n$  1890); (c) PPG ( $M_n$  2180); (d) EPH2.

and third steps between 350 and 433 °C (Figure 4d). In comparison with the TGA curves of pure PHB-diol and pure PEG, the first weight loss step is attributed to the decomposition of PHB segment and the second and third weight loss step to the decomposition of both the PEG and PPG segments. However, the second and third weight loss steps are too close for the accurate determination of the compositions of PPG and PEG separately. Therefore, only the PHB content of EPH2 could be determined from the degradation profile. Similar weight loss curves were also observed for other poly(PEG/PPG/PHB urethane)s. The PHB contents estimated from TGA results are in good agreement with those calculated from  $^1\text{H}$  NMR.

**Critical Micellization Concentration (CMC) Determination.** Among the six poly(PEG/PPG/PHB urethane)s, only EPH1, EPH2, EPH3, and EPH5 were soluble in water. The CMC determination was carried out for these four copolymers. This experiment was conducted by varying the aqueous polymer concentration in the range of 0.0001 to 0.5 wt %, while keeping the concentration of DPH constant. DPH shows a higher absorption coefficient in a hydrophobic environment than in water. Thus, with increasing polymer concentration, the absorbances at 344, 358, and 378 nm increased (Figure 5a). The point where the absorbance suddenly increases corresponds to the concentration at which micelles are formed. When the micelle is formed, DPH partitions preferentially into the hydrophobic core formed in the aqueous solution.<sup>22a,27–29</sup> The CMC was determined by extrapolating the absorbance at 378 nm minus the absorbance at 400 nm ( $A_{378} - A_{400}$ ) versus logarithmic concentration (Figure 5b). The CMC values for the water-soluble copolymers are tabulated in Table 1 and are in the range of  $5.16 \times 10^{-4}$  to  $9.79 \times 10^{-4}$  g.mL $^{-1}$ . Comparing the copolymers of similar molecular weights, the CMC values are much lower than that reported by Ahn et al. for a series of multiblock PEG-PPG-PEG copolymers,<sup>19</sup> showing that the incorporation of PHB greatly increases the hydrophobicity of the copolymers, resulting in a decrease in the CMC values.

$^{13}\text{C}$  NMR was used to investigate the effect of solvent on the micelle structure.<sup>29,31–34</sup>  $\text{CDCl}_3$  is a good nonselective solvent for PHB, PEG, and PPG while water is a good selective solvent for PEG but poor for PPG and PHB. As shown in Figure 6, in  $\text{CDCl}_3$ , the peaks due to the PHB, PEG, and PPG were sharp and well defined. In  $\text{D}_2\text{O}$ , PEG is shown as a sharp peak but the PHB and the PPG peaks are collapsed and broadened. This shows that the molecular motion of PHB and PPG is slow in water, indicating a hydrophobic core structure made up of PHB and PPG with PEG as the outer corona structure, confirming the core-corona structure of the micelle.<sup>31–33</sup> However, in the light of the multiblock architecture of the copoly-

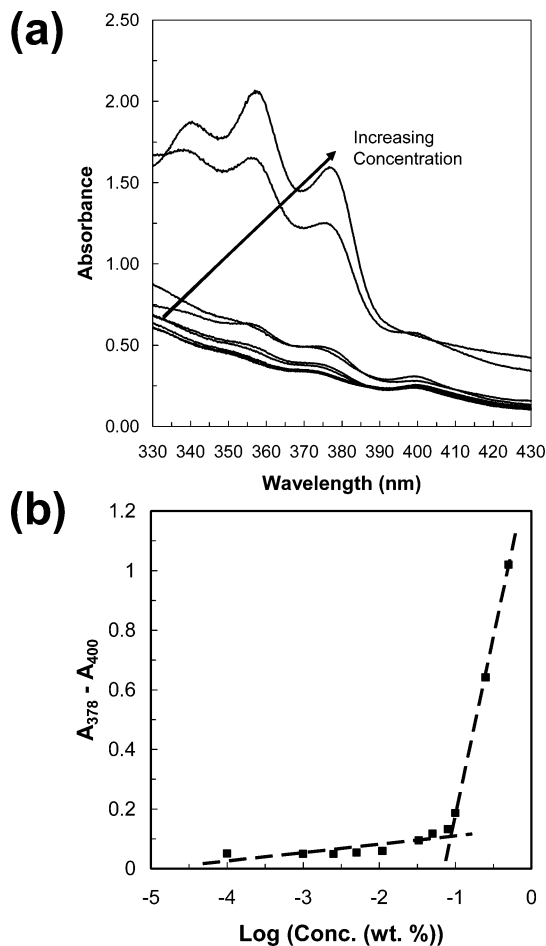


**Figure 5.** (a) UV-vis spectra changes of DPH with increasing EPH2 copolymer concentration in water at 25 °C. DPH concentration was fixed at 6 mM, and the polymer concentration varied between 0.0001 and 0.5 wt %. The increase in the absorbance band at 378 nm indicates the formation of a hydrophobic environment in water. (b) CMC determination by extrapolation of the difference in absorbance at 378 and 400 nm.

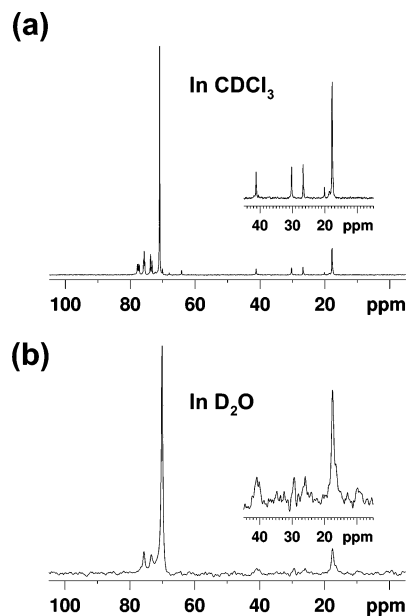


**Figure 6.**  $^{13}\text{C}$  NMR spectra of EPH2 (5 wt %) in (a)  $\text{CDCl}_3$  and (b)  $\text{D}_2\text{O}$  at 25 °C.

mers, it is not reasonable to expect that the simple micelles of an ABA-type amphiphilic polymer be formed. Instead, it would

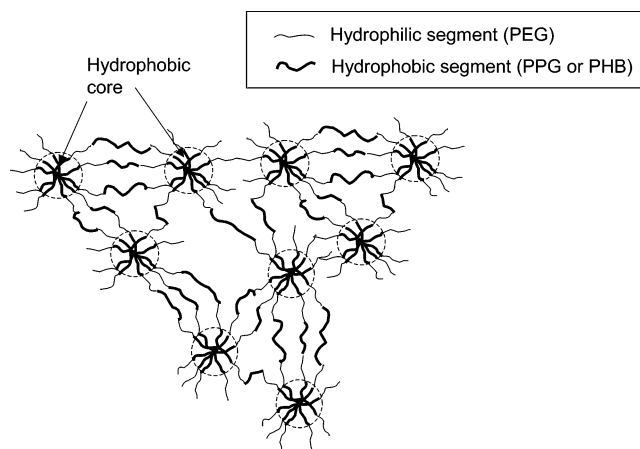


**Figure 7.** Associated micelle model showing the network-like packing of the polymer chains.

be more plausible to consider an associated micelle model in the consideration of the above results. An associated micelle structure could be formed by the network-like packing of the polymer chains, as illustrated in Figure 7.

#### Thermoreversible Sol–Gel Transition of the Copolymers.

The phase diagrams of the poly(ester urethane)s in aqueous solutions were determined by the test tube inverting method.<sup>22a,29</sup> The results are shown in Figure 8. Three regions can be identified from the diagram, the lower soluble region, gel region, and the upper soluble region. As the temperature increased monotonically from 4 to 80 °C, the aqueous polymer solution underwent a sol–gel–sol transition. It is noted that the reverse transition also took place upon cooling from 80 to 4 °C. The critical gelation concentration (CGC) is defined as the minimum copolymer concentration in aqueous solution at which the gelation behavior could be observed. The CGCs of the copolymers in this work were found to be between 2 and 5 wt %. These values are much lower than that reported for many thermogelling copolymers.<sup>19–22,28–30,32,35</sup> Examining the gelation properties of the EPH series of copolymers, it appears that the incorporation of a small amount of PHB led to a decrease in CGC (EPH1 → EPH2). However, upon further addition of PHB, the CGC increased (EPH2 → EPH3).

The changes of the molecular environment occurring during the sol–gel transition of a 5 wt % EPH2 solution in D<sub>2</sub>O was monitored by <sup>13</sup>C NMR technique at different temperatures (Figure 9). At low temperatures where the copolymer was a solution, the peaks ascribed to the PEG, PPG, and PHB segments were sharp and well defined because the segments interacted freely with the solvent molecules in the solution. At higher temperatures where the copolymer formed a hydrogel, the peaks were collapsed and broadened as compared with those observed at low temperatures. The phenomena can be attributed to the lower dynamic motion of the copolymer segments in the gel state.<sup>22a,28,29,31–33,36</sup> Due to the network-like packing of the multiblock polymer chains, the motion of all the components in the copolymer became restricted to a certain extent. Upon further increase in the temperature to 75 °C, the turbid sol state was obtained, and the PEG, PPG, and PHB peaks were consequently seen as sharp and well defined again, which indicates that there was an increase in molecular motion of the PEG, PPG, and PHB blocks, possibly due to phase mixing between the blocks. Additionally, this reflects the disruption of the core-corona structure and an exposure of the hydrophobic core to the aqueous environment.<sup>31,36</sup> It has been reported that PEG dissolved in aqueous solution becomes dehydrated at higher temperatures.<sup>37</sup> Furthermore, the hydrodynamic radius

of PEG in water decreases with an increase in temperature.<sup>38</sup> PPG has also been reported to be less soluble in water at elevated temperatures.<sup>39</sup> As the copolymer was made up of more than 60 wt % of PEG, it is reasonable to expect that any change in the properties of PEG segments would significantly affect the properties of the copolymer. At the turbid sol state, there could be significant dehydration of the PEG segments, leading to a phase separation between the polymer and water. The decrease of the hydrodynamic radius of the copolymer was largely influenced by the dehydration of PEG. This brought the different segment blocks closer together, resulting in a collapse in the copolymer structure. There could then be possible phase mixing between the segments. PEG has been demonstrated to be a solvent for PHB at elevated temperatures.<sup>40</sup> Thus, it was possible that the PEG, PPG, and PHB segments form a homogeneous mixture which was phase separated from the aqueous solution. Upon phase separation, the core-corona structure was disrupted and consequently the hydrophobic core was exposed to the aqueous environment.<sup>32</sup> The turbid sol was made up of particulate matter with the sizes ranging from a few to tens micrometers (see Supporting Information). Overall, the <sup>13</sup>C NMR technique has offered insights on the packing mechanism at the molecular level for the gel–sol transition process.

The viscosities of the hydrogels were studied as a function of temperature. In general, the transition temperature corresponded well with the transition temperature determined using the test tube inverting method. The viscosity of the gels at 5 °C was between 50 and 200 cP, corresponding to a fluidic sol state. Figure 10 shows that as the concentration of EPH2 in aqueous solution increased, the viscosity of the gel increased. It is interesting to note that at the critical gelation concentration of EPH2 (2 wt %), the hydrogel displayed a higher maximum viscosity (43 000 cP) than a hydrogel containing 20 wt % EG<sub>100</sub>-PG<sub>65</sub>EG<sub>100</sub> triblock polymer gel (33 000 cP). The result clearly shows that the gels of this work are more robust than that of the PEG-PPG-PEG triblock copolymer gel. Above 3 wt %, the EPH2 gels attained a maximum viscosity of more than 55 000 cP. The increased viscosity of the gels allowed long-term sustained release of the model protein drug using bovine serum albumin (BSA). Preliminary studies showed that sustained release of up to 70 days was achievable with our system. Further details will be published in an upcoming manuscript.

**Proposed Sol–Gel Transition Mechanism.** From the collated results of the micellar and gelation studies, we can propose a sol–gel transition mechanism for the multiblock copolymer system as follows. The amphiphilic block copolymers form associated micelles at concentrations in the region of 0.1 wt %. These micelles comprise the hydrophobic PPG and PHB core and the hydrophilic PEG corona that interacts with the water molecules. Upon increasing the concentration up to above 2 wt %, the thermoresponsive copolymers exist as a solution at low temperatures, but undergo a reversible phase transition from a clear solution to a clear gel, and further to a turbid sol upon increase in temperature from 4 to 80 °C. From a solution state at low temperatures, a monotonic increase in temperature causes the PEG segments to become slightly dehydrated.<sup>37</sup> PPG segments also become less soluble in water with increasing temperatures.<sup>39</sup> These changes provide the driving forces for the micellar aggregation when the hydrophobicity and hydrophilicity of the system achieves a balanced state. The PEG corona would self-associate instead of interacting with the neighboring water molecules, forming micelle aggregates.<sup>38</sup> As the micelle aggregates form a close packed structure, a gel state is observed. Further increase in temperature leads to a significant

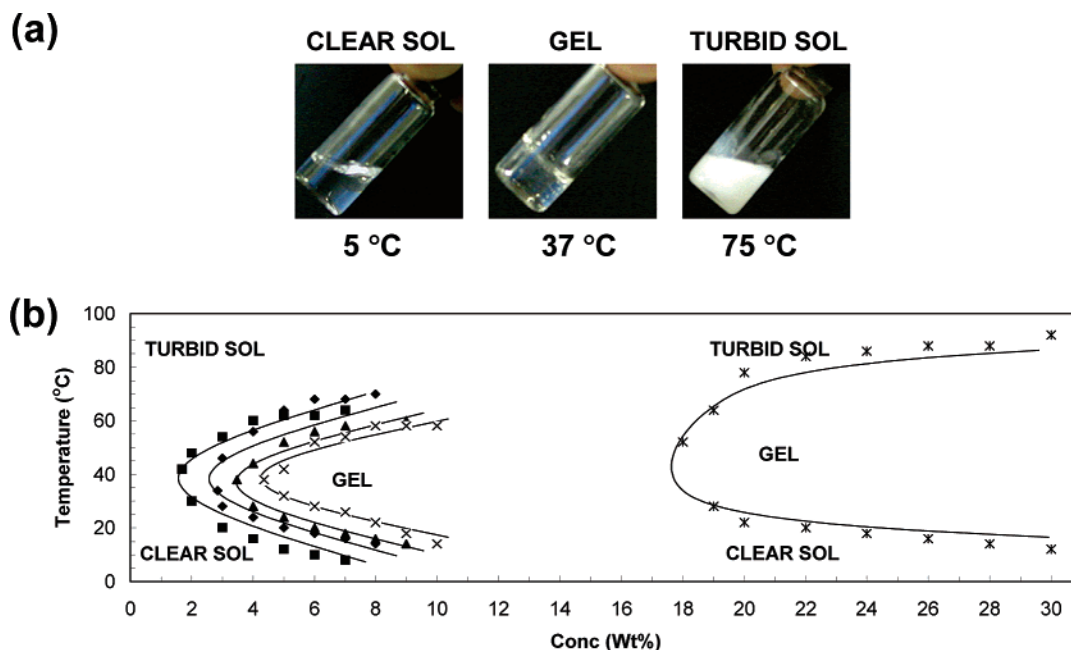


**Figure 8.** (a) Graphics showing the gel transition of poly(PHB/PEG/PEG urethanes) (EPH2: 5 wt % in H<sub>2</sub>O) with increasing temperature. The transition from a clear sol to a gel and further to a turbid sol is observed in the graphics. (b) Sol-gel phase diagrams of poly(PEG/PPG/PHB urethanes) in aqueous solutions in comparison with EG<sub>100</sub>PG<sub>65</sub>EG<sub>100</sub> triblock polymer (▲, EPH1; ■, EH2; ◆, EPH3; ×, EPH5; \*, EG<sub>100</sub>PG<sub>65</sub>EG<sub>100</sub>).

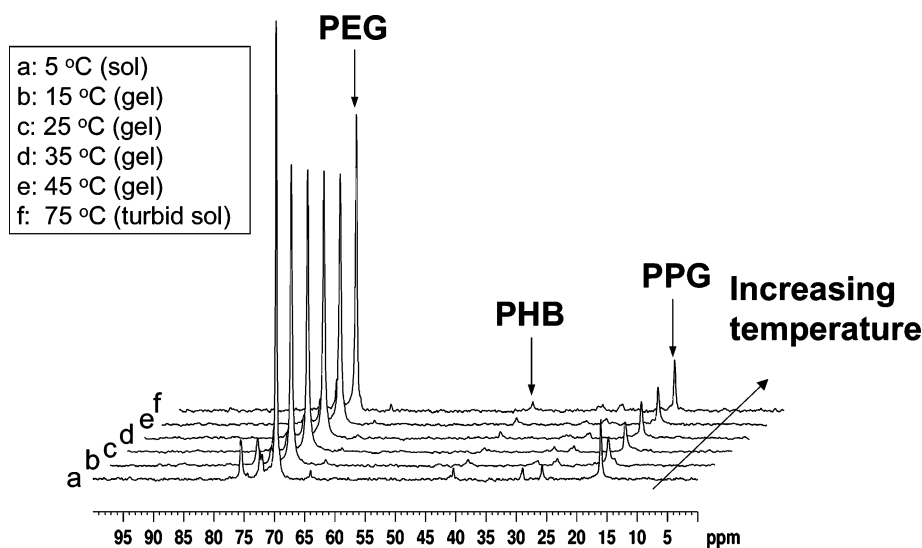


**Figure 9.** <sup>13</sup>C NMR of EPH2 in D<sub>2</sub>O (5 wt %) at different temperatures.

dehydration and the eventual collapse of the PEG corona.<sup>38</sup> Phase mixing of PEG, PPG, and PHB segments takes place due to the favorable interactions between the polymer segments of different blocks. The phase separation of the polymeric components from the aqueous solution results in the disruption of the core-corona structure and exposes the hydrophobic core to the aqueous environment.<sup>31,36</sup> This leads to the formation of a fluidic turbid sol at high temperatures.

These multiblock copolymer gels possess lower CMCs and CGCs than the widely studied thermogelling copolymers with the triblock chain architecture. This could be in part due to the increased association of the micelles brought about by the multiple segments that link the micelles together in a network-like structure. These segmental links facilitate the micellar aggregation process by reducing the degree of freedom possessed by the individual micelles. Cohn et al. developed a series of PEG/PPG/PCL multiblock copolymers which showed higher

CGCs as compared with PEG/PPG multiblock copolymers.<sup>21</sup> This was attributed to the spatial effect of the caprolactone segments, which affects the packing of the polymer chains. In this work, we observed that the CGC value of the copolymer is very sensitive to the amount of PHB incorporated into the copolymers. Comparing EPH1 and EPH2, both having very low PHB levels, the effect of the spatial hindrances due to the PHB segments were superseded by the strong hydrophobic interaction between the PHB segments. However, a further increase in the PHB content increased the CGC of the copolymer (EPH3), reflecting the spatial effect of the PHB segment on the packing of the polymer chains (Figure 8). Comparing the CGC values of EPH3 and EPH5 (3 wt % and 6 wt %, respectively), the copolymers having similar PHB content but different PHB block lengths, it appears that longer PHB segments would lead to a greater spatial hindrance and thus lead to a higher CGC value. This shows that the block length and the content



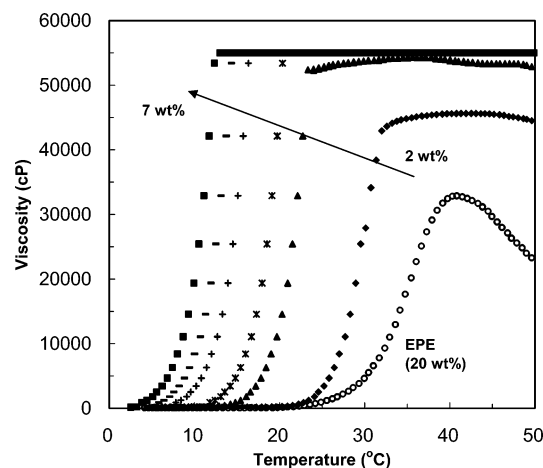


**Figure 10.** Viscosity as a function of temperature for EPH2 in aqueous solution at different concentrations  $\blacklozenge$ , 2 wt %;  $\blacktriangle$ , 3 wt %;  $*$ , 4 wt %;  $+$ , 5 wt %;  $-$ , 6 wt %;  $\blacksquare$ , 7 wt % in comparison with EG<sub>100</sub>-PG<sub>65</sub>-EG<sub>100</sub> triblock copolymer (O, EPE, 20 wt %) at the shear rate of 9.6 s<sup>-1</sup>.

of PHB incorporated into the copolymer could be utilized as parameters in the control of the properties of the thermogelling copolymers.

### Conclusions

Potentially biodegradable and biocompatible poly(PEG/PPG/PHB urethanes), with PEG and PPG molar ratios fixed at 2:1 and various amounts of PHB, have been successfully synthesized using HDI as a coupling agent. Their chemical structure and molecular characteristics were studied with GPC, <sup>1</sup>H NMR, <sup>13</sup>C NMR, and FTIR, which confirmed the architecture of the random multiblock poly(PEG/PPG/PHB urethanes). The GPC results indicated that the synthesized poly(PEG/PPG/PHB urethanes) had high molecular weights with relatively narrow molecular weight distributions. The contents of PHB segments in the copolymers calculated from <sup>1</sup>H NMR ranged from 2.1 to 12.7 wt %. It was found that the incorporation of 11.4 wt % of PHB and above rendered the poly(PEG/PPG/PHB urethanes) insoluble in water.

The thermal stability of the poly(PEG/PPG/PHB urethanes) was studied by TGA, and three separate thermal degradation steps corresponding to PHB, PPG, and PEG segments were observed, from which the PHB contents were calculated. The results were in good agreement with those from the <sup>1</sup>H NMR measurements. The poly(PEG/PPG/PHB urethanes) presented better thermal stability than the PHB precursors.

The CMC values of the water-soluble copolymers were determined by the dye solubilization method. The CMC values of the copolymers in this work ranged from  $5.16 \times 10^{-4}$  to  $9.79 \times 10^{-4}$  g mL<sup>-1</sup>. On the basis of the dye solubilization and <sup>13</sup>C NMR experiments, the micelles are concluded to have a hydrophobic core made up of PHB and PPG segments and an outer hydrophilic corona of PEG segments.

The sol-gel transitions of the aqueous copolymers were studied, and phase diagrams showing the various sol and gel regions as a function of temperature and concentration of the solution was generated. The critical gelation concentration of the copolymers in this work ranged from 2 to 5 wt %. From the <sup>13</sup>C NMR spectra of the copolymers at various temperatures, the sol-gel transition can be elucidated at a molecular level. The viscosities of the EPH2 gel at various concentrations were studied and were found to be much higher than the gel formed

by the EG<sub>100</sub>PG<sub>65</sub>EG<sub>100</sub> triblock copolymer (20 wt %). From the collated experimental results of the micellar and gelation studies as well as consideration of the multiblock architecture of the copolymers, we propose an associated micelle packing mechanism for the sol-gel transition for the copolymers at increasing temperatures.

**Acknowledgment.** The authors acknowledge the financial support from the Agency for Science, Technology and Research (A\*STAR), Singapore, and the National University of Singapore. The authors thank M. J. Loh and J. G. Lim for kindly proof-reading the manuscript. X. J. Loh would like to acknowledge the National Science Scholarship from A\*STAR.

**Supporting Information Available.** Additional experimental procedures and images of EPH1, EPH2, and EPH3 gels at 20 and 80 °C. This material is available free of charge via the Internet at <http://pubs.acs.org>.

### References and Notes

- Huang, K.; Lee, B. P.; Ingram, D. R.; Messersmith, P. B. *Biomacromolecules* **2002**, *3*, 397–406.
- Daga, A.; Muraglia, A.; Quarto, R.; Cancedda, R.; Corte, G. *Gene Ther.* **2002**, *9*, 915–921.
- Packhaeuser, C. B.; Schnieders, J.; Oster, C. G.; Kissel, T. *Eur. J. Pharm. Biopharm.* **2004**, *58*, 445–455.
- Heller, J.; Barr, J.; Ng, S. Y.; Shen, H. R.; Abdellaoui, S.; Gurny, R.; Castioni, N. V.; Loup, P. J.; Baehni, P.; Mombelli, A. *Biomaterials* **1999**, *23*, 4397–4404.
- Hill-West, J. L.; Chowdhury, S. M.; Slepian, M. J.; Hubbell, J. A. *Proc. Natl. Acad. Sci. U.S.A.* **1994**, *91*, 5967–5971.
- Yokoyama, M. *Crit. Rev. Ther. Drug Carrier Syst.* **1992**, *9*, 213–248.
- Gilbert, J. C.; Hadgraft, J.; Bye, A.; Brookes, L. *Int. J. Pharm.* **1986**, *32*, 223–228.
- Nalbandian, R. M.; Henry, R. L.; Wilks, H. S. *J. Biomed. Mater. Res.* **1972**, *6*, 583–590.
- Exner, A. A.; Krupka, T. Y.; Scherrer, K.; Teets, J. M. *J. Controlled Release* **2005**, *106*, 188–197.
- Esposito, E.; Carotta, Y.; Scabbia, A.; Trombelli, L.; D'Antona, P.; Menegatti, E.; Nastruzzi, C. *Int. J. Pharm.* **1996**, *142*, 9–23.
- Katakam, M.; Ravis, W. R.; Golden, D. L.; Banga, A. K. *Int. J. Pharm.* **1997**, *152*, 53–58.
- Blonder, J. M.; Baird, L.; Fulfs, J.; Rosenthal, G. J. *Life Sci.* **1999**, *65*, 261–266.
- Wout, Z. G. M.; Pec, E. A.; Maggiore, J. A.; Williams, R. H.; Palicharla, P.; Johnston, T. P. *J. Parent. Sci. Technol.* **1992**, *46*, 192–200.
- Palmer, W. K.; Emeson, E. E.; Johnston, T. P. *Atherosclerosis* **1998**, *136*, 115–123.
- Ho, A. K.; Bromberg, L.; Huibers, P. D. T.; O'Connor, A. J.; Perera, J. M.; Stevens, G. W.; Hatton, T. A. *Langmuir* **2002**, *18*, 3005–3013.
- Cleary, J.; Bromberg, L.; Magner, E. *Langmuir* **2002**, *19*, 9162–9172.
- Bromberg, L. *Ind. Eng. Chem. Res.* **1998**, *37*, 4267–4274.
- Bromberg, L. *J. Phys. Chem. B* **1998**, *102*, 10736–10744.
- Ahn, J. S.; Suh, J. M.; Lee, M.; Jeong, B. *Polym. Int.* **2005**, *54*, 842–847.
- Cohn, D.; Sosnik, A.; Levy, A. *Biomaterials* **2003**, *24*, 3707–3714.
- Cohn, D.; Sosnik, A. *Biomaterials* **2005**, *26*, 349–357.
- (a) Hwang, M. J.; Suh, J. M.; Bae, Y. H.; Kim, S. W.; Jeong, B. *Biomacromolecules* **2005**, *6*, 885–890. (b) Jeong, B.; Bae, Y. H.; Kim, S. W. *J. Controlled Release* **2000**, *63*, 155–163. (c) Jeong, B.; Bae, Y. H.; Lee, D. S.; Kim, S. W. *Nature* **1997**, *388*, 860–862.
- (a) Li, J.; Li, X.; Ni, X. P.; Leong, K. W. *Macromolecules* **2003**, *36*, 2661–2667. (b) Li, J.; Ni, X. P.; Li, X.; Tan, N. K.; Lim, C. T.; Ramakrishna, S.; Leong, K. W. *Langmuir* **2005**, *21*, 8681–8685. (c) Li, X.; Mya, K. Y.; Ni, X. P.; He, C.; Leong, K. W.; Li, J. *J. Phys. Chem. B* **2006**, *110*, 5920–5926.
- Li, X.; Loh, X. J.; Wang, K.; He, C.; Li, J. *Biomacromolecules* **2005**, *6*, 2740–2747.
- Loh, X. J.; Tan, K. K.; Li, X.; Li, J. *Biomaterials* **2006**, *27*, 1841–1850.



- (26) Loh, X. J.; Wang, X.; Li, H.; Li, X.; Li, J. *Mater. Sci. Eng. C*, in press.
- (27) Alexandridis, P.; Holzwarth, J. F.; Hatton, T. A. *Macromolecules* **1994**, *27*, 2414–2425.
- (28) Bae, S. J.; Suh, J. M.; Sohn, Y. S.; Bae, Y. H.; Kim, S. W.; Jeong, B. *Macromolecules* **2005**, *38*, 5260–5265.
- (29) Jeong, B.; Bae, Y. H.; Kim, S. W. *Macromolecules* **1999**, *32*, 7064–7069.
- (30) Behraves, E.; Shung, A. K.; Jo, S.; Mikos, A. G. *Biomacromolecules* **2002**, *3*, 153–158.
- (31) Jeong, B.; Bae, Y. H.; Kim, S. W. *Colloids Surf. B: Biointerfaces* **1999**, *16*, 185–193.
- (32) Jeong, B.; Windisch, C. F., Jr.; Park, M. J.; Sohn, M. J.; Gutowska, A.; Char, K. *J. Phys. Chem. B* **2003**, *107*, 10032–10039.
- (33) Lee, B. H.; Lee, Y. M.; Sohn, Y. S.; Song, S. C. *Macromolecules* **2002**, *35*, 3876–3879.
- (34) Durand, A.; Hourdet, D.; Lafuma, F. *J. Phys. Chem. B* **2000**, *104*, 9371–9377.
- (35) Booth, C.; Attwood, D. *Macromol. Rapid. Commun.* **2000**, *21*, 501–527.
- (36) Jeong, B.; Kibbey, M. R.; Birnbaum, J. C.; Won, Y. Y.; Gutowska, A. *Macromolecules* **2000**, *33*, 8317–8322.
- (37) Harris, J. M. *Poly(ethylene glycol) Chemistry*; Plenum Press: New York, 1993; pp 263–268.
- (38) Jeong, B. Ph.D. Thesis, University of Utah, 1999.
- (39) Yu, M.; Nishiumi, H.; Arons, J. S. *Fluid Phase Equilib.* **1993**, *83*, 357–364.
- (40) Ravenelle, F.; Marchessault, R. H. *Biomacromolecules* **2002**, *3*, 1057–1064.

BM0607933